0026-895X/94/020317-07$03.00/0

MOLECULAR PHARMACOLOGY, 45:317-323

The Agonist Binding Site of the γ-Aminobutyric Acid Type A Channel Is Not Formed by the Extracellular Cysteine Loop

JAHANSHAH AMIN, IAN M. DICKERSON, and DAVID S. WEISS

Department of Physiology and Biophysics and The Institute for Biomolecular Science, University of South Florida College of Medicine, Tampa, Florida 33612-4799 (J.A., D.S.W.), and Department of Physiology and Biophysics, University of Miami School of Medicine, Miami, Florida 33101 (I.M.D.)

Received September 13, 1993; Accepted November 29, 1993

SUMMARY

The amino-terminal extracellular domain of the subunits comprising the γ-aminobutyric acid (GABA) receptor contains two cysteine residues (designated at relative positions 1 and 15) separated by 13 amino acids. These two cysteines (presumably disulfide bonded) are located approximately 150 amino acids from the amino terminus. There is significant homology in the amino acid sequence of this cysteine loop both between the different subunits of the GABA receptor and with subunits of other members of this ligand-gated ion channel superfamily (nicotinic acetylcholine- and glycine-activated ion channels). A number of highly conserved amino acids within the cysteine loop have been postulated to play a role in agonist binding. Here, using site-directed mutagenesis and oocyte expression, we have examined the effects of mutating amino acids comprising the cysteine loop on the activation of recombinant GABA channels composed of rat α1, β2, and γ2 subunits. Preventing the formation of the putative cysteine-cysteine disulfide bond in any of the subunits, by mutating the cysteine at position 15 to serine, prevented the functional expression of that subunit. For example, coexpression of γ_{C15S} with wild-type α and β subunits resulted in GABA-activated currents with properties identical to those of GABA-activated currents from coexpression of α and β subunits alone. These properties included sensitivity to activation by GABA (similar EC_{50} values), blockade by Zn^{2+}, and lack of modulation by the benzodiazepine diazepam. We also mutated conserved amino acids in the β subunit that had been specifically proposed to form the GABA binding site (β_{R6}, β_{Y8}, and β_{D11}). These mutations (as well as several others within or adjacent to the cysteine loop) produced either a very moderate effect or no effect on GABA sensitivity, suggesting that these particular amino acids do not play a key role in activation of the GABA channel. The data presented in this study support a role for the cysteine loop in subunit assembly, rather than channel activation.

The GABA-activated chloride channel is a member of a receptor-operated ion channel superfamily that also includes the nACh- and glycine-activated ion channels (1–3). The subunits comprising these presumably pentameric (4–6) receptor/ion channels display significant sequence homology and share several structural features, such as four putative membrane-spanning domains (M1-M4), a long and sequence-variable intracellular loop between M3 and M4, and a large amino-terminal extracellular domain. In addition, all subunit isoforms identified thus far contain a cysteine loop in the same approximate position of the amino-terminal extracellular domain. The cysteine loop consists of two disulfide-bonded cysteine residues separated by 13 amino acids.

The striking conservation of several amino acids within the cysteine loop motif in all known subunit isoforms of the nACh, GABA, and glycine channels has drawn considerable attention to this domain as being potentially important for channel function. More specifically, it has been proposed that the amphiphillic cysteine loop may form part of the agonist binding site (7, 8). In support of this proposal, a synthetic peptide corresponding to residues 125–147 (with the cysteines at positions 128 and 142 being disulfide bonded) of the nACh channel α subunit binds ACh and the competitive antagonist α-bungarotoxin (9). Modeling studies of the ligand-binding pocket based on agonist structure and a comparative amino acid sequence analysis of all subunit isoforms postulate specific amino acids within the cysteine loop essential for agonist binding to nACh-, glycine-, and GABA-activated ion channels (10–12). What role the cysteine loop plays in agonist-dependent gating of the GABA channel, however, is still unclear.

We have been using site-directed mutagenesis and oocyte expression to examine the effects of mutations in the cysteine loop on the activation of recombinant GABA channels composed of rat α1, β2, and γ2 subunits. Here we present evidence

This research was supported by a grant from the Alcohol, Drug Abuse, and Mental Health Association to D.S.W. and an Initial Investigatorship Award from the American Heart Association (Florida Affiliate) to I.M.D.

ABBREVIATIONS: GABA, γ-aminobutyric acid; HEPES, 4-(2-hydroxyethyl)-1-piperazineethanesulfonic acid; PCR, polymerase chain reaction; ACh, acetylcholine; nACh, nicotinic acetylcholine.

that suggests that the cysteine loop does not form a crucial component of the agonist binding site. Although some mutations within the cysteine loop did slightly impair activation of the GABA channel, evidence suggests that this impairment may occur indirectly through structural alterations of the protein. Finally, preventing the formation of the disulfide bond of the cysteine loop in either the $\alpha 1$, $\beta 2$, or $\gamma 2$ subunits prevented the functional expression of the mutated subunit, suggesting that the cysteine loop may be required for proper subunit folding or association. Preliminary observations of this study have previously appeared in abstract form (13).

Materials and Methods

Isolation of GABA channel subunit cDNAs. Based on the published sequences (14–17), we used the PCR to isolate cDNAs encoding the $\alpha 1$, $\beta 2$, and $\gamma 2$ subunits from total RNA. Total RNA was isolated from rat brain using standard procedures (18) and was then reverse transcribed using the downstream PCR oligonucleotide as a primer. The upstream and downstream primers were as follows: $\alpha 1$ upstream, 5′-*GCG***AAGCTT**GACCATGAAGAAAAGTCGGGG-3′; $\alpha 1$ downstream, 5′-*CGG***TCTAGA**GTGCAGAGGACTGAACAAACG-3′; $\beta 2$ upstream, 5′-*GCG***GTCGAC**GACCATGTGGAGAGTCCGGAA-3′; $\beta 2$ downstream, 5′-*CGG***GGATCC**GTTTGAAGAGGAATCTA-3′; $\gamma 2$ upstream, 5′-*GCG***AAGCTT**GACCATGAGTTCGCCAAATAC-3′; $\gamma 2$ downstream, 5′-*CGG***TCTAGA**CCCAAACCTCCTCACAGATAA-3′. Sequences in italics are "GC clamps" to prevent the ends of the PCR product from flaring during cloning procedures, sequences in bold type are restriction sites (*Hind*III and *Xba*I for $\alpha 1$ and $\gamma 2$ and *Sal*I and *Bam*HI for $\beta 2$), and underlined bases are Kozak sequences to enhance translation (19). Standard procedures were used for the PCR (20). The amplified cDNAs were cloned into the pSP72 vector using the engineered restriction sites and sequenced (21) until a clone was found that matched the published amino acid sequence.

Site-directed mutagenesis and *in vitro* transcription. cDNAs were cloned into the pSELECT vector (Promega, Madison WI) and oligonucleotide-mediated site-directed mutagenesis was achieved with Altered Sites (Promega). Successful mutagenesis was verified by sequencing.

cDNAs were linearized with *Ssp*I, which leaves a several-hundred-base pair tail that may increase cRNA stability in the oocyte. cRNA was transcribed from the linearized cDNAs by standard *in vitro* transcription procedures or Megascript (Ambion, Austin TX).

Oocyte isolation and cRNA injection. *Xenopus laevis* (Xenopus I, Ann Arbor MI) were anesthetized by hypothermia and oocytes were surgically removed from the frog and placed in OR2, which consisted of 82.5 mM NaCl, 2.5 mM KCl, 10 mM HEPES, 2 mM $CaCl_2$, 1 mM $MgCl_2$, 10 mM Na_2HPO_4, 50 units/ml penicillin, and 50 μg/ml streptomycin, pH 7.5. Oocytes were dispersed in OR2 without Ca^{2+} with 0.3% collagenase A (Boehringer Mannheim, Indianapolis IN). After isolation, the oocytes were thoroughly rinsed with OR2. Stage VI oocytes were separated and maintained overnight at 18°.

Micropipettes for injecting cRNA were fabricated on a Sutter P87 horizontal puller and the tips were cut off with microscissors. cRNAs for the desired subunit combinations were mixed (in equal ratios), diluted 5–30-fold with diethylpyrocarbonate-treated water, and drawn up into the micropipette with negative pressure. The cRNA was injected into the oocytes by application of positive pressure using a Picospritzer II (General Valve Corporation, Fairfield, NJ). A different micropipette was used for each cRNA combination, to prevent the possibility of cRNA cross-contamination.

To ensure that equal concentrations of cRNA for each construct were injected (especially important for comparison of maximum GABA-activated currents), *in vitro* synthesized cRNAs, at different fixed dilutions, were electrophoresed on a 1% formaldehyde-containing agarose gel. The amount of cRNA was judged and matched by interpolation of lanes containing different dilutions of the corresponding cRNA.

Electrophysiology. One to 3 days after injection, oocytes were placed on a 300-μm nylon mesh suspended in a small-volume chamber (<100 μl). The chamber had an inlet in the top and an outlet in the bottom, which allowed continuous perfusion. Eighteen separate reservoirs (50-ml syringe barrels) were connected to three six-way valves, and the outlet of each of these six-way valves was connected to one four-way valve. The outlet of the four-way valve led to the chamber. The four-way valve gated between the three banks of six reservoirs and the six-way valve controlled the individual reservoirs within a bank of six. In this way, up to 18 different solutions could be introduced to an individual oocyte. Switching between the different solutions was controlled manually. The oocyte was continuously perfused with OR2 (without antibiotics and with 10 mM Na_2HPO_4 replaced with 10 mM NaCl) and briefly switched to the test solution containing GABA. Applications of high concentrations of agonist were separated by several minutes, to reduce desensitization. To test and correct for cumulative desensitization, the same nondesensitizing concentration of agonist was applied after every two test applications (correction procedure explained below).

Recording microelectrodes were fabricated with a P87 Sutter horizontal puller and filled with 3 M KCl. They had resistances of 1–3 MΩ. Standard two-electrode voltage-clamp techniques (9050A Oocyte Clamp; Knight Industrial Technologies, Miami FL) were used to record currents in response to application of agonist. In all cases, the membrane potential was clamped to −70 mV. Data were monitored with a Gould EasyGraf chart recorder during the experiment and recorded with a videocassette recorder (Instrutech 10b) for off-line analysis.

Data analysis. Peak current amplitudes were measured directly from the chart record. The following equation was used to correct the current amplitudes for cumulative desensitization:

$$I_{corrected} = I_{observed} \cdot \frac{I_0}{I_j} \quad (1)$$

where $I_{observed}$ is the recorded current, I_0 is the current amplitude in response to the first application of the control concentration of agonist, and I_j is the current amplitude in response to the control application preceding the particular test application. This correction was only necessary at high agonist concentrations and usually changed $I_{observed}$ by <20%. Equation 1 corrects only for cumulative desensitization and does not correct for fast components of desensitization that occur before the peak and would produce an underestimation of the peak amplitude.

With high levels of GABA channel expression (maximum GABA-activated currents of >2.5 μA), the EC_{50} was shifted slightly to the left. With lower levels of expression, normalized dose-response curves were very reproducible between experiments even when the maxima were very different. Therefore, data presented in this report were limited to oocytes that displayed a maximum current of <2.5 μA.

To quantify the agonist sensitivity, each dose-response relationship was fitted with the following equation using a nonlinear least squares method:

$$I = \frac{I_{max}}{1 + (EC_{50}/[A])^n} \quad (2)$$

where I is the peak current at a given concentration of agonist A, I_{max} is the maximum current, EC_{50} is the concentration of agonist yielding half-maximal current, and n is the Hill coefficient. For measurements comparing maximum GABA-activated currents, GABA was applied at a concentration ≈10-fold higher than the EC_{50} for that particular subunit combination.

Results

This study examined GABA-activated chloride currents from oocytes expressing various combinations of wild-type and mu-

tant α1, β2, and γ2 subunits (henceforth designated simply as α, β, and γ). Fig. 1A shows the aligned amino acid sequences of the α, β, and γ subunits for the cysteine loop and flanking regions. For ease of reference, the amino acids comprising the cysteine loop of all three subunits are numbered 1 through 15, starting at the first cysteine of each isoform. (Conversion factors for the actual amino acid positions are given in the legend to Fig. 1.) Fig. 1B shows the approximate location of the cysteine loop in a diagram of the putative membrane topology of the GABA channel subunits (3). The cysteine loop is located ≈150 amino acids from the amino terminus and ≈70 amino acids from the first membrane-spanning domain.

Note in Fig. 1A that several cysteine loop amino acids are conserved in the α, β, and γ subunits, namely the leucine at position 5, the proline at position 9, and the aspartic acid at position 11. These three amino acids are also conserved in all other identified α, β, γ, and δ subunit isoforms. Several other positions, although not identical, show conservative variability, such as position 3 (hydrophobic), position 8 (aromatic), and position 10 (hydrophobic). The amphiphillic nature of the cysteine loop and its conservation of several amino acids between subunit isoforms have been cited as supporting evidence for a role of the cysteine loop in ligand binding (8, 11, 12).

Mutations that prevent the formation of the putative disulfide bond. Fig. 2A shows GABA-activated currents, at several representative concentrations of GABA, from an oocyte expressing wild-type α, β, and γ subunits. Fig. 2B, *squares*, plot the peak of the currents (normalized to the maximum) versus GABA concentration (data averaged from five oocytes). Fig. 2B, *solid line through the squares*, shows an average of the best fit of the Hill equation to the individual dose-response relationships, which yielded an EC_{50} (concentration required for half-maximal activation) of 45.8 ± 3.6 μM and a Hill coefficient of 1.59 ± 0.09 (Table 1).

We next prevented the formation of the presumed disulfide bond of the cysteine loop (3), in each subunit, by mutating the cysteine at position 15 to serine (Fig. 1A). For each mutant subunit, cRNA was transcribed from the cDNA and injected,

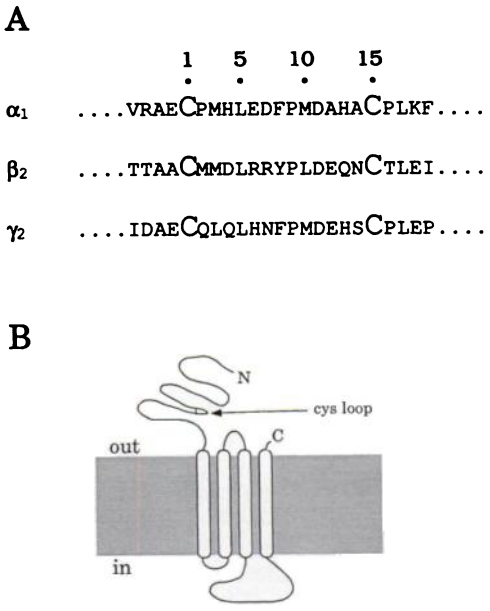

Fig. 1. Amino acid sequence of the α1, β2, and γ2 cysteine loops and the location of the cysteine loop with respect to the putative membrane topology of the GABA subunits. A, The single-letter amino acid sequences are given for the α1, β2, and γ2 subunits. For ease of reference, the amino acids have been numbered 1 through 15. For conversion to the proper amino acid positions, add 137, 135, and 150 to the indicated numbers for α1, β2, and γ2, respectively. B, The cysteine loop is located in the large amino-terminal extracellular region ≈70 amino acids from the first membrane-spanning domain.

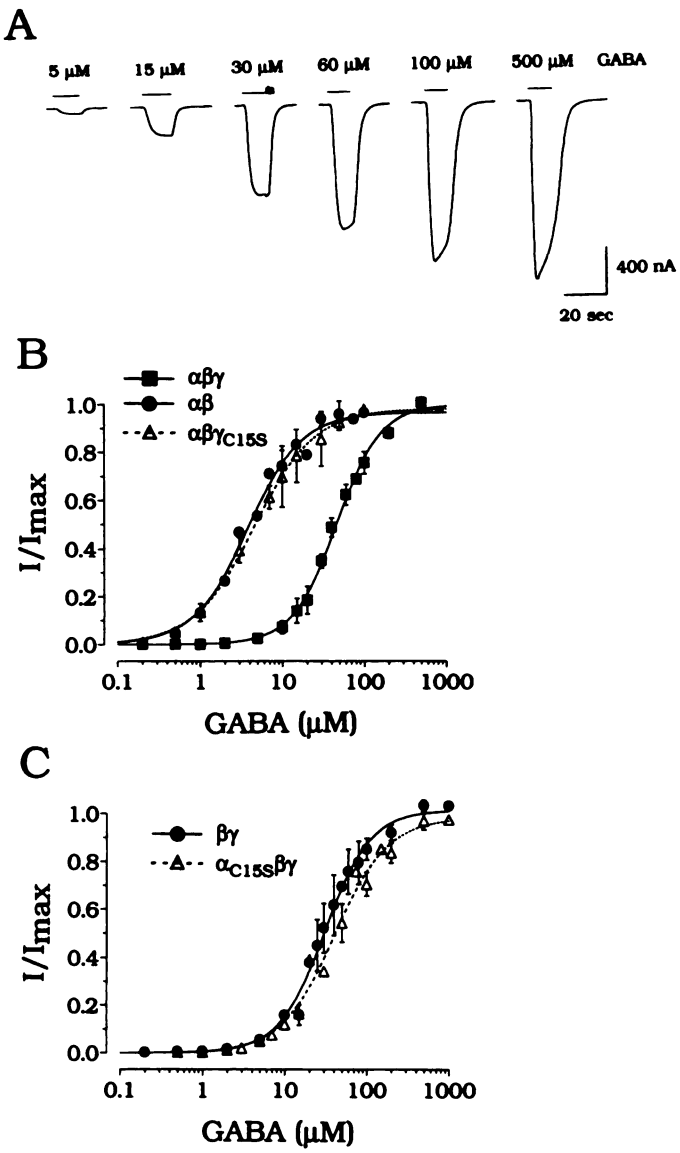

Fig. 2. The dose-response relationship for GABA-activated currents from oocytes injected with α, β, and γ_{C15S} cRNAs was identical to the dose-response relationship seen with coexpression of α and β subunits alone. A, GABA-activated currents from an oocyte expressing $\alpha\beta\gamma$ (wild-type) GABA channels. Currents are shown at six representative GABA concentrations. *Bars above the currents*, duration of oocyte exposure to GABA. B, Peak GABA-activated currents measured at several GABA concentrations and normalized to the maximum for each oocyte. *Points*, means ± standard deviations for five, three, and four oocytes for $\alpha\beta\gamma$, $\alpha\beta$, and $\alpha\beta\gamma_{C15S}$ coexpression, respectively. *Solid and dashed lines*, best fits of the data using the Hill equation, as described in Materials and Methods. The parameters of the fits are listed in Table 1. Note that the activation properties of the GABA-activated currents in oocytes injected with $\alpha\beta$ and $\alpha\beta\gamma_{C15S}$ cRNA combinations are indistinguishable. C, Peak GABA-activated currents measured at several GABA concentrations and normalized to the maximum for each oocyte. *Points*, means ± standard deviations for five and three oocytes for $\beta\gamma$ and $\alpha_{C15S}\beta\gamma$ coinjections, respectively. *Solid and dashed lines*, best fits of the data using the Hill equation, as described in Materials and Methods.

TABLE 1

Parameters determined from fitting the Hill equation to dose-response relationships, as described in Materials and Methods

All EC_{50} and Hill coefficient values are means ± standard deviations. Combinations for which no GABA-activated currents were observed were tested with concentrations of GABA of 10,000 μM or greater. Mutations $\beta_{RR6,7KK}$ and $\beta_{RR6,7NS}$ each represent two point mutations. $I_{max\text{-}mut}/I_{max\text{-}wt}$ is the ratio of the maximum GABA-activated current of the mutant to the maximum GABA-activated current of the wild-type receptor. The maxima were determined, in a separate set of experiments, by injection of equal amounts of cRNA for the different subunit combinations and application of GABA at a concentration ≈ 10 times the EC_{50}.

Combination	EC_{50}	Hill coefficient	No. of oocytes tested	$I_{max\text{-}mut}/I_{max\text{-}wt}$ (n)
	μM			
$\alpha\beta\gamma$	45.8 ± 3.6	1.59 ± 0.09	5	1.0 ± 0.26 (5)
$\alpha\beta$	4.2 ± 0.9	1.23 ± 0.12	3	
$\beta\gamma$	30.1 ± 8.4	1.51 ± 0.09	5	
$\alpha\gamma$	No GABA-activated currents observed		4	
$\alpha\beta_{D4N}\gamma$	31.2 ± 2.4	1.46 ± 0.07	4	
$\alpha\beta_{L5O}\gamma$	No GABA-activated currents observed		4	
$\alpha\beta_{L5M}\gamma$	272.9 ± 16.5	1.29 ± 0.09	3	0.03 ± 0.03 (5)
$\alpha\beta_{L5O}\gamma$	547.8 ± 162.8	1.06 ± 0.10	3	
$\alpha\beta_{R6K}\gamma$	126.8 ± 24.8	1.38 ± 0.14	3	0.78 ± 0.25 (5)
$\alpha\beta_{R6N}\gamma$	119.1 ± 3.9	1.29 ± 0.00	3	0.28 ± 0.20 (3)
$\alpha\beta_{R6E}\gamma$	158.3 ± 9.1	1.21 ± 0.09	3	0.22 ± 0.07 (5)
$\alpha\beta_{RR6,7KK}\gamma$	149.2 ± 29.5	1.47 ± 0.11	5	
$\alpha\beta_{RR6,7NS}\gamma$	190.6 ± 48.3	1.35 ± 0.14	12	
$\alpha\beta_{Y8F}\gamma$	17.2 ± 3.6	1.72 ± 0.38	3	
$\alpha\beta_{Y8S}\gamma$	No GABA-activated currents observed		10	
$\alpha\beta_{D11N}\gamma$	No GABA-activated currents observed		13	
$\alpha\beta_{D11E}\gamma$	44.5 ± 3.8	0.88 ± 0.08	3	0.003 ± 0.002 (6)
$\alpha\beta_{E12D}\gamma$	69.1 ± 20.5	1.30 ± 0.12	2	
$\alpha\beta_{E12Q}\gamma$	62.3 ± 15.3	1.22 ± 0.04	2	
$\alpha\beta\gamma_{C15S}$	5.06 ± 1.53	1.15 ± 0.18	3	
$\beta\gamma_{C15S}$	No GABA-activated currents observed		7	
$\alpha_{C15S}\beta\gamma$	46.5 ± 11.6	1.24 ± 0.3	3	
$\alpha_{C15S}\beta$	No GABA-activated currents observed		5	
$\alpha\beta_{C15S}\gamma$	No GABA-activated currents observed		3	
$\alpha\beta_{T16A}\gamma$	173.1 ± 45.1	1.36 ± 0.17	4	0.06 ± 0.04 (5)
$\alpha\beta_{L17Q}\gamma$	No GABA-activated currents observed		3	
$\alpha\beta_{L17D}\gamma$	No GABA-activated currents observed		4	
$\alpha\beta_{L17M}\gamma$	No GABA-activated currents observed		6	
$\alpha_{D11E}\beta\gamma$	16.0 ± 3.9	1.38 ± 0.15	3	
$\alpha\beta\gamma_{D11E}$	26.8 ± 3.3	1.60 ± 0.09	3	

along with its wild-type counterpart cRNAs, into oocytes. Coexpression of the γ_{C15S} subunit (cysteine at position 15 of the γ subunit replaced with serine) with wild-type α and β subunits resulted in robust GABA-activated currents. Fig. 2B, *triangles*, plot the average dose-response relationship (three oocytes) for coinjection of α, β, and γ_{C15S} cRNAs. Fig. 2B, *dashed line*, shows an average of the best fit of the Hill equation to the individual dose-response relationships, which yielded an EC_{50} of 5.1 ± 1.5 μM and a Hill coefficient of 1.15 ± 0.18 (Table 1).

There are four lines of evidence suggesting that γ_{C15S} was not functionally present when coexpressed with wild-type α and β subunits. First, the activation properties for GABA-activated currents with α, β, and γ_{C15S} cRNA coinjection were indistinguishable from the activation properties with coexpression of α and β alone (compare Fig. 2B, *circles* and *triangles*; also see parameters in Table 1). Second, coinjection of γ_{C15S} and β cRNAs did not result in the expression of GABA-activated currents, whereas coexpression of the β subunit with the wild-type γ subunit did result in functional GABA channels (Table 1). Individual injections of α, β, or γ cRNAs in oocytes did not result in GABA-activated currents (22).[1]

The third line of evidence suggesting that the γ_{C15S} subunit was not functionally present when coinjected with wild-type α and β cRNAs was demonstrated by examining Zn^{2+} blockade (23, 24). GABA-activated currents (3 μM GABA) from oocytes expressing only α and β subunits were almost completely blocked by 10 μM Zn^{2+} (Fig. 3, *top*). As demonstrated in Fig. 3, *middle*, only a small component of the current from α, β, and γ coexpression was blocked by Zn^{2+} (25.7 ± 4.9%; $n = 7$). [The fraction of the current in $\alpha\beta\gamma$-expressing oocytes blocked by Zn^{2+} may represent the Zn^{2+}-blockable subpopulation of $\alpha\beta$ (23) and $\beta\gamma$[1] subunit combinations.] Thus, the presence of the γ subunit prevented Zn^{2+} blockade of the GABA channels. Fig. 3, *bottom*, demonstrates that, similar to coexpression of α and β subunits alone, GABA-activated currents from oocytes coinjected with α, β, and γ_{C15S} cRNAs were almost completely blocked by 10 μM Zn^{2+}.

Finally, the fourth line of evidence suggesting the functional absence of the γ_{C15S} subunit was derived by examining benzodiazepine potentiation of GABA-activated currents. The presence of the γ subunit is required for potentiation of GABA-

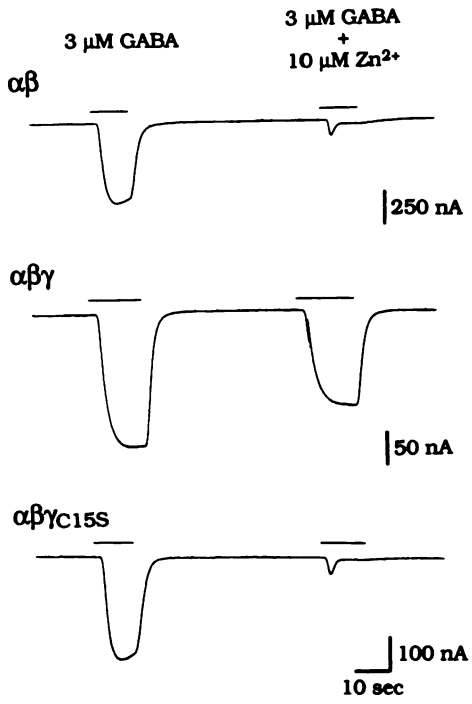

Fig. 3. Zn^{2+} blocks GABA-activated currents from oocytes injected with α, β, and γ_{C15S} cRNAs. GABA-activated currents were examined in response to application of 3 μM GABA, applied alone or coapplied with 10 μM Zn^{2+}. GABA-activated currents from oocytes expressing only α and β subunits were blocked by 10 μM Zn^{2+} (*top*). Coexpression of α, β, and γ subunits yielded GABA-activated currents that were only partially blocked by Zn^{2+} (*middle*). As was true for α and β coexpression alone, GABA-activated currents resulting from coinjection of α, β, and γ_{C15S} cRNAs were blocked by Zn^{2+} (*bottom*).

[1] J. Amin, I. M. Dickerson, and D. S. Weiss, unpublished observations.

activated currents by benzodiazepines (25). GABA-activated currents from oocytes coinjected with α, β, and γ_{C15S} cRNAs, as was true for $\alpha\beta$ coexpression, were not potentiated by the benzodiazepine diazepam (1 μM), whereas 1 μM diazepam potentiated GABA-activated currents from the $\alpha\beta\gamma$ subunit combination by ≈3.4-fold (336 ± 28%; n = 3 oocytes; data not shown).

We also examined the C15S mutant of the α subunit. Coinjection of α_{C15S}, β, and γ cRNAs resulted in GABA-activated currents with activation properties similar to those of the $\beta\gamma$ subunit combination (Fig. 2C; Table 1). Fig. 2C, *circles*, show normalized dose-response relationships for oocytes expressing β and γ subunits (five oocytes) and Fig. 2C, *triangles*, show normalized dose-response relationships for oocytes coinjected with α_{C15S}, β, and γ cRNAs (three oocytes). Because the $\beta\gamma$ activation properties were similar to the $\alpha\beta\gamma$ activation properties (Table 1), the data in Fig. 2C did not provide evidence on the absence or presence of the mutant α subunit. However, coinjection of α_{C15S} and β cRNAs did not yield GABA-activated currents (Table 1), suggesting the functional absence of the α_{C15S} subunit.

Finally, we tested the C15S mutant of the β subunit. Coinjection of α, β_{C15S}, and γ cRNAs resulted in no GABA-activated currents, as was true for coinjection of wild-type α and γ cRNAs (Table 1).

The data presented in this section suggest that preventing the formation of the disulfide bond in either the α, β, or γ subunit prevented the functional expression of that subunit. This suggests that the cysteine loop may be required for proper folding or assembly of the subunits in the plasma membrane. These data, however, do not preclude a role for the cysteine loop in activation of the GABA channel.

Mutations of amino acids within the cysteine loop postulated to form part of the agonist binding site. Evidence from photoaffinity labeling studies suggests that the major components of the GABA binding site reside on the β subunit (26, 27). Modeling studies based on the structure of GABA and an amino acid sequence analysis of the cysteine loop region propose specific residues within the β subunit cysteine loop that interact with GABA (12). More specifically, the arginine at position 6 (β_{R6}) has been postulated to interact with the carboxylate group of the GABA molecule, whereas the aspartic acid at position 11 (β_{D11}) has been postulated to interact with the amino group of GABA. In addition, the β subunit of the GABA channel is distinct from all other isoforms in this receptor-operated superfamily, in that it contains a tyrosine, rather than a phenylalanine, at position 8 (β_{Y8}). This tyrosine has been proposed to form a side-chain hydrogen bond with β_{R6} that optimizes the position of the arginine for interaction with GABA. We tested this model of the agonist binding site by examining the effects of mutation of β_{R6}, β_{Y8}, and β_{D11} on agonist-mediated activation.

The arginine at position 6 of the β subunit cysteine loop was substituted with lysine (β_{R6K}), asparagine (β_{R6N}), or glutamic acid (β_{R6E}). Fig. 4A shows dose-response relationships for wild-type and β_{R6} mutants and Fig. 4B plots the EC_{50} values determined for $\alpha\beta\gamma$, $\alpha\beta_{R6K}\gamma$, $\alpha\beta_{R6N}\gamma$, and $\alpha\beta_{R6E}\gamma$ subunit combinations. All three mutations resulted in a ≈3-fold increase in the EC_{50}, compared with the wild-type receptor (Table 1), and produced a modest depression in the maximum GABA-activated current (Table 1).

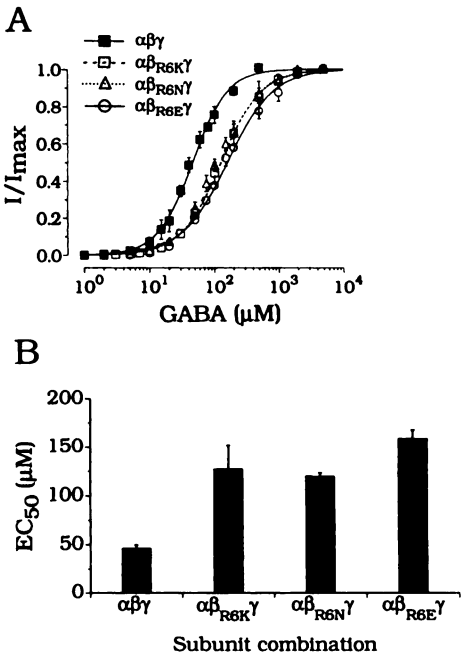

Fig. 4. Mutation of β_{R6} produced a very moderate, and charge-independent, decrease in GABA sensitivity. A, Peak currents were measured at several GABA concentrations and normalized to the maximum current, as in Fig. 2. *Points*, means ± standard deviations for five wild-type and three mutant oocytes. *Solid*, *dashed*, and *dotted lines*, best fits of the data using the Hill equation, as described in Materials and Methods. The parameters from these fits are listed in Table 1. B, The means ± standard deviations of the EC_{50} values for channels with substitutions at β_{R6} are shown. The moderate decrease in GABA sensitivity did not correlate with the charge at this position.

The three substitutions presented in Fig. 4 were conservative in terms of hydrophilicity. In addition, the β_{R6K} substitution was conservative in terms of charge (positive), whereas the β_{R6N} and β_{R6E} mutations replaced the positive charge at this position with a neutral and negative charge, respectively. The data in Fig. 4 demonstrate that the shift in EC_{50} for the mutants did not correlate with the charge substituted at this position.

Conservative substitutions of amino acids forming the binding sites of ACh-, glycine-, and GABA-operated ion channels typically yield EC_{50} increases of at least 10-fold, whereas less conservative substitutions typically abolish agonist-dependent gating (28–32). Therefore, the lack of correlation between the shift in EC_{50} and the amino acid substitution at β_{R6}, coupled with the relatively minor shifts in EC_{50}, suggests that β_{R6} does not form a crucial component of the agonist binding site. Furthermore, the observed depression in the maximum GABA-activated current suggests that the mutations may affect channel assembly or gating.

We next substituted the tyrosine at position 8 with a phenylalanine (β_{Y8F}), which would prevent the formation of the proposed side-chain hydrogen bond between β_{R6} and β_{Y8} (12). As shown in Table 1, this mutation did not impair activation of the GABA channel by GABA. In fact, the sensitivity to GABA activation was increased by ≈3-fold and there was a concomitant increase in the Hill coefficient. We also substituted a serine at this position (β_{Y8S}) (Table 1). Although this mutation conserved the hydroxyl group, no functional GABA-activated currents were observed when β_{Y8S} was coinjected with wild-type α and γ cRNAs. The much smaller size of serine, however, may impose steric constraints on the region sufficient

to disrupt the cysteine loop structure and prevent channel function or assembly.

Mutation of β_{D11} to asparagine (β_{D11N}) and coinjection with wild-type α and γ cRNAs resulted in no GABA-activated currents (Table 1). The more conservative mutation (in terms of charge) to glutamic acid (β_{D11E}) did produce GABA-activated currents. This substitution did not affect the EC_{50} but, interestingly, decreased the Hill coefficient, suggesting a decrease in the cooperativity of channel activation. Such an effect on the Hill coefficient with no alteration in the EC_{50} is incompatible with a simple effect on agonist binding. Moreover, there was a dramatic decrease in the maximum GABA-activated current with the β_{D11E} mutant (Table 1), suggesting a significant disruption in channel assembly and/or gating.

The aspartic acid at position 11 is also conserved in the α and γ subunits. We mutated these corresponding aspartic acids to glutamic acid and coexpressed these mutant α and γ subunits with their wild-type counterparts. GABA-activated currents were then measured to determine the EC_{50} values for the $\alpha_{D11E}\beta\gamma$ and $\alpha\beta\gamma_{D11E}$ subunit combinations. As shown in Table 1, GABA-mediated activation was not impaired in either case (in fact, there was a very slight decrease in the EC_{50} values), suggesting that these conserved amino acids do not play a crucial role in agonist-mediated activation of the GABA channel. In conclusion, site-directed mutagenesis of β_{R6}, β_{Y8}, and β_{D11} suggests that the GABA binding site model proposed by Cockcroft *et al.* (12), at least in its present form, is unlikely.

Mutations of other amino acids in the β subunit cysteine loop. We have also examined the effects of mutating other amino acids in the β subunit cysteine loop on GABA-mediated activation. The substitutions β_{D4N}, β_{R7N}, β_{R7S}, β_{E12D}, and β_{E12Q} all had negligible effects on sensitivity to GABA (Table 1), suggesting that these amino acids do not play a crucial role in GABA-mediated activation. On the other hand, substitutions of β_{L5} did decrease the apparent sensitivity to GABA (Table 1). The conservative substitution β_{L5M} increased the EC_{50} value 6-fold, whereas the less conservative substitution β_{L5Q} increased the EC_{50} value 12-fold. Furthermore, substitution of β_{L5} with aspartic acid prevented the formation of functional GABA channels. The increase in EC_{50} for β_{L5M} was also associated with a >30-fold decrease in the maximum GABA-activated current (Table 1). This decrease in the maximum current is incompatible with a simple effect of the mutation on agonist binding and may represent a disruption of channel assembly and/or gating. Finally, we have tested the effects of mutating the threonine at position 16 and the leucine at position 17 (both just outside the cysteine loop). β_{T16A} produced an only moderate increase (3-fold) in the EC_{50} and a significant depression (17-fold) in the maximum current (Table 1). All substitutions tested thus far at β_{L17} (β_{L17M}, β_{L17Q}, and β_{L17D}) prevented the formation of functional GABA channels (Table 1), suggesting that this leucine may play a crucial structural role.

Discussion

Cockcroft *et al.* (12), using comparative molecular modeling, proposed that the extracellular cysteine loop forms a type VIA hairpin turn, with residues 1–7 and 10–14 forming opposing β-strands. In their model β_{D11}, through a charge interaction, binds the amino group of the GABA molecule while β_{R6} interacts with the carboxyl group of GABA. Proper positioning of β_{R6} is accomplished by side-chain hydrogen bonding between β_{R6} and β_{Y8}.

This study was designed to test the role of the cysteine loop in agonist-mediated activation of the GABA channel and, more specifically, to test the hypothesis that the cysteine loop forms part of the GABA binding site. To this end, we examined the effects of mutating β_{R6}, β_{Y8}, and β_{D11} on GABA-mediated activation. Although our experiments do not measure GABA binding directly, substitution of residues critical for agonist binding would be evident as a rightward shift in the dose-response relationship for GABA-activated currents.

Substitution of β_{R6} decreased the sensitivity to GABA by ≈3-fold. This 3-fold shift in sensitivity was observed regardless of the charge of the amino acid substituted at this position. Because conservative mutations of amino acids crucial for agonist binding usually decrease agonist sensitivity by 1 order of magnitude or more, whereas nonconservative mutations typically abolish agonist-mediated activation, we conclude that β_{R6} does not contribute a crucial component of the agonist binding site. We also substituted phenylalanine for β_{Y8}, which would prevent the formation of the proposed side-chain hydrogen bond with β_{R6}. This substitution did not decrease the sensitivity to activation by GABA. Finally, substitution of β_{D11} with glutamic acid did not increase the EC_{50}, although it did decrease the Hill coefficient and the maximum GABA-activated current. Single-channel analysis is underway to gain insight into the mechanism by which this mutation affects the cooperativity of activation.

Mutations of other amino acids within the cysteine loop (β_{D4}, β_{R7}, and β_{E12}) produced very little effect on the agonist sensitivity. Substitution of β_{L5} with methionine and glutamine, however, produced a 6- and 12-fold decrease in efficacy, respectively. These decreases in efficacy were associated with dramatic reductions in the peak current, consistent with an impairment of channel assembly or of the coupling between agonist binding and gating of the pore (32).

It should be mentioned that mutations could affect fast components of desensitization (which would go undetected in these studies), thereby producing an apparent decrease in agonist sensitivity. A detailed electrophysiological examination of the effects of these mutations on desensitization is better carried out in transfected mammalian cells or membrane patches, where a more rapid application of agonist can be achieved.

How do our results compare with what is known about the role the cysteine loop plays in the function of other members of this receptor-operated superfamily? Mutation of the position 6 lysine (homologous to β_{R6}) and the position 11 aspartic acid in the homomeric glycine receptor did not impair sensitivity to activation by glycine (33). Studies using monoclonal antibodies directed to the cysteine loop region of the nACh channel concluded that the cysteine loop does not form part of the agonist binding site (34, 35). Mishina *et al.* (36) prevented the formation of the disulfide bond in the α subunit of the nACh channel and observed no ACh-activatable currents (but see Ref. 37). They proposed that the cysteine loop motif may be required for proper assembly of the subunit. Along similar lines, Sumikawa and Gehle (37) observed that disruption of the disulfide loop structure in the nACh channel α or β subunits led to intracellular retention of the assembled receptor com-

plexes, suggesting that the cysteine loop may be required for efficient transport of the receptors to the plasma membrane.

Our data, in part, agree with these observations, in that mutations that prevented the formation of the disulfide bond of the cysteine loop prevented the functional expression of that particular subunit. Furthermore, mutations of several amino acids in or around the cysteine loop produced a decrease in the maximum GABA-activated current, suggesting a possible impairment of channel assembly. However, the decrease in the maximum current was sometimes associated with a decrease in agonist sensitivity (β_{R6}, β_{L5}, and β_{T17}), suggesting that these mutations did not simply result in assembly impairment (i.e., they also altered channel function). The decrease in agonist sensitivity could result from an alteration in protein structure that indirectly affected agonist binding (i.e., the cysteine loop may help shape the binding pocket). Alternatively, the cysteine loop domain may play a role in the transduction mechanism between agonist binding and channel opening. This mechanism could account for both the increase in EC_{50} and the decrease in the maximum current. Nevertheless, studies on the nACh and glycine receptors, and now the GABA receptor, suggest that it is unlikely that the cysteine loop forms a crucial component of the agonist binding site in this family of receptor-operated ion channels.

Acknowledgments

The authors wish to recognize the technical assistance of Mike Madden and Sonal Barot.

References

1. Noda, M., H. Takahashi, T. Tanabe, M. Toyosato, Y. Furutani, T. Hirose, H. Takashima, S. Inayama, T. Miyata, and S. Numa. Structural homology of *Torpedo californica* acetylcholine receptor subunits. *Nature (Lond.)* **302**:528–531 (1983).
2. Greeningloh, G., A. Rienitz, B. Schmitt, C. Methfessel, M. Zensen, K. Beyreuther, E. D. Gundelfinger, and H. Betz. The strychnine-binding subunit of the glycine receptor shows homology with the nicotinic acetylcholine receptors. *Nature (Lond.)* **328**:215–220 (1987).
3. Schofield, P. R., M. G. Darlison, N. Fujita, D. R. Burt, F. A. Stephenson, H. Rodriguez, L. M. Rhee, J. Ramachandran, V. Reale, T. A. Glencorse, P. H. Seeburg, and E. A. Barnard. Sequence and functional expression of the $GABA_A$ receptor shows a ligand-gated receptor super-family. *Nature (Lond.)* **328**:221–227 (1987).
4. Langosch, D., L. Thomas, and H. Betz. Conserved quaternary structure of ligand-gated ion channels: the postsynaptic glycine receptor is a pentamer. *Proc. Natl. Acad. Sci. USA* **85**:7394–7398 (1988).
5. Cooper, E., S. Couturier, and M. Ballivet. Pentameric structure and subunit stochiometry of a neuronal nicotinic acetylcholine receptor. *Nature (Lond.)* **350**:235–238 (1991).
6. DeLorey, T. M., and R. W. Olsen. γ-Aminobutyric $acid_A$ receptor structure and function. *J. Biol. Chem.* **267**:16747–16750 (1992).
7. Noda, M., H. Takahashi, T. Tanabe, M. Toyosato, Y. Furutani, T. Hirose, H. Takashima, S. Inayama, T. Miyata, and S. Numa. Primary structure of *alpha*-subunit precursor of *Torpedo californica* acetylcholine receptor deduced from cDNA sequence. *Nature (Lond.)* **299**:793–797 (1992).
8. Barnard, E. A., M. G. Darlison, and P. H. Seeburg. Molecular biology of the $GABA_A$ receptor channel superfamily. *Trends Neurosci.* **10**:502–509 (1987).
9. McCormick, D. J., and M. Z. Attassi. Localization and synthesis of the acetylcholine-binding site in the α-chain of *Torpedo californica* acetylcholine receptor. *Biochem. J.* **224**:995–1000 (1984).
10. Smart, L., H.-W. Meyers, R. Hilgenfeld, W. Saenger, and A. Maelicke. A structural model for the ligand-binding site at the nicotinic acetylcholine receptor. *FEBS Lett.* **178**:64–68 (1984).
11. Luyten, W. H. M. L. A model for the acetylcholine binding site of the nicotinic acetylcholine receptor. *J. Neurosci. Res.* **16**:61–73 (1986).
12. Cockcroft, V. B., D. J. Osguthorpe, E. A. Barnard, and G. G. Lunt. Modeling of agonist binding to the ligand-gated ion channel superfamily of receptors. *Proteins Struct. Funct. Genes* **8**:386–397 (1990).
13. Amin, J., and D. S. Weiss. Mutations which effect agonist-dependent gating of the $GABA_A$-activated chloride channel. *Biophys. J.* **64**:326A (1992).
14. Khrestchatisky, M., A. J. MacLennan, M.-Y. Chiang, W. Xu, M. B. Jackson, N. Brecha, C. Sternini, R. W. Olsen, and A. J. Tobin. A novel α subunit in rat brain $GABA_A$ receptors. *Neuron* **3**:745–753 (1989).
15. Lolait, S. J., A. M. O'Carroll, K. Kusano, J.-M. Muller, M. J. Brownstein, and L. C. Mahan. Cloning and expression of a novel rat $GABA_A$ receptor. *FEBS Lett.* **246**:145–148 (1989).
16. Shivers, B. D., I. Killisch, R. Sprengel, H. Sontheimer, M. Kohler, P. R. Schofield, and P. H. Seeburg. Two novel $GABA_A$ receptor subunits exist in distinct neuronal subpopulations. *Neuron* **3**:327–337 (1989).
17. Ymer, S., P. R. Schofield, A. Draguhn, P. Werner, M. Kohler, and P. H. Seeburg. $GABA_A$ receptor β subunit heterogeneity: functional expression of cloned cDNAs. *EMBO J.* **8**:1665–1670 (1989).
18. Sambrook, J., E. F. Fritsch, and T. Maniatis. *Molecular Cloning: A Laboratory Manual*, Vol. 1. Cold Spring Harbor Laboratory, Cold Spring Harbor, NY (1989).
19. Kozak, M. Point mutations define a sequence flanking the AUG initiator codon that modulates translation by eukaryotic ribosomes. *Cell* **44**:283–292 (1986).
20. Saiki, R. K., D. H. Gelfand, D. H. Stoffel, S. J. Scharf, R. Higuchi, G. T. Horn, K. B. Mullis, and H. A. Erlich. Primer directed enzyme amplification with a thermostable DNA polymerase. *Science (Washington D. C.)* **239**:487–491 (1988).
21. Sanger, F., S. Nicklen, and A. R. Coulson. DNA sequencing with chain terminating inhibitors. *Proc. Natl. Acad. Sci. USA* **74**:5463–5467 (1977).
22. Sigel, E., R. Baur, G. Trube, H. Mohler, and P. Malherbe. The effect of subunit composition of rat brain $GABA_A$ receptors on channel function. *Neuron* **5**:703–711 (1990).
23. Draguhn, A., T. A. Verdoorn, M. Ewert, P. H. Seeburg, and B. Sakmann. Functional and molecular distinction between recombinant rat $GABA_A$ receptor subtypes by Zn^{2+}. *Neuron* **5**:781–788 (1990).
24. Legendre, P., and G. L. Westbrook. Noncompetitive inhibition of γ-aminobutyric $acid_A$ channels by Zn^{2+}. *Mol. Pharmacol.* **39**:267–274 (1991).
25. Pritchett, D. B., H. Sontheimer, B. D. Shivers, S. Ymer, H. Kettenmann, P. R. Schofield, and P. H. Seeburg. Importance of a novel $GABA_A$ receptor subunit for benzodiazepine pharmacology. *Nature (Lond.)* **338**:582–585 (1989).
26. Casalotti, S. O., A. Stephenson, and E. A. Barnard. Separate subunits for agonist and benzodiazepine binding in the γ-aminobutyric $acid_A$ receptor oligomer. *J. Biol Chem.* **261**:15013–15016 (1986).
27. Deng, L., R. W. Ransom, and R. W. Olsen. [^{3}H]Muscimol photolabels the γ-aminobutyric acid receptor binding site on a peptide subunit distinct from that labelled with benzodiazepine. *Biochem. Biophys. Res. Commun.* **138**:1308–1314 (1986).
28. Galzi, J. L., D. Bertrand, A. Devillers-Thiery, F. Revah, S. Bertrand, and J.-P. Changeux. Functional significance of aromatic amino acids from three peptide loops of the α_7 neuronal nicotinic receptor site investigated by site-directed mutagenesis. *FEBS Lett.* **294**:198–202 (1991).
29. O'Leary, M. E., and M. M. White. Mutational analysis of ligand-induced activation of the *Torpedo* acetylcholine receptor. *J. Biol. Chem.* **267**:8360–8365 (1992).
30. Tomaselli, G. F., J. T. McLaughlin, M. E. Juman, E. Hawrot, and G. Yellen. Mutations affecting agonist sensitivity of the nicotinic acetylcholine receptor. *Biophys. J.* **60**:721–727 (1991).
31. Vandenberg, R. J., C. A. Handford, and P. R. Schofield. Distinct agonist- and antagonist-binding sites on the glycine receptor. *Neuron* **9**:491–496 (1992).
32. Amin, J., and D. S. Weiss. $GABA_A$ receptor needs two homologous domains of the β-subunit for activation by GABA but not by pentobarbital. *Nature (Lond.)* **366**:565–569 (1993).
33. Vandenberg, R. J., S. Rajendra, S. R. French, P. H. Barry, and P. R. Schofield. The extracellular disulfide loop motif of the inhibitory glycine receptor does not form the agonist binding site. *Mol. Pharmacol.* **44**:198–203 (1993).
34. Lennon, V. A., D. J. McCormick, E. H. Lambert, G. E. Griesmann, and M. Z. Atassi. Region of peptide 125–147 of acetylcholine receptor α subunit is exposed at neuromuscular junction and induces experimental autoimmune myasthenia gravis, T-cell immunity, and modulating autoantibodies. *Proc. Natl. Acad. Sci. USA* **82**:8805–8809 (1985).
35. Criado, M., V. Sarin, J. L. Fox, and J. Lindstron. Evidence that the acetylcholine binding site is not formed by the sequence α127–143 of the acetylcholine receptor. *Biochemistry* **25**:2839–2846 (1986).
36. Mishina, M., T. Tobimatsu, K. Imoto, K. Tanaka, Y. Fujita, K. Fukuda, M. Kurasaki, H. Takahashi, Y. Morimoto, T. Hirose, S. Inayama, T. Takahashi, M. Kuno, and S. Numa. Location of functional regions of acetylcholine receptor α-subunit by site-directed mutagenesis. *Nature (Lond.)* **313**:364–369 (1985).
37. Sumikawa, K., and V. M. Gehle. Assembly of mutant subunits of the nicotinic acetylcholine receptor lacking the conserved disulfide loop structure. *J. Biol. Chem.* **267**:6286–6290 (1992).

Send reprint requests to: David S. Weiss, Department of Physiology and Biophysics, MDC Box 8, University of South Florida College of Medicine, 12901 Bruce B. Downs Blvd., Tampa, FL 33612–4799.